Controlled Self-Assembly

DOI: 10.1002/anie.200803361

Controlled Self-Assembly Manipulated by Charge-Transfer Interactions: From Tubes to Vesicles**

*Chao Wang, Shouchun Yin, Senlin Chen, Huaping Xu, Zhiqiang Wang, and Xi Zhang**

Molecular self-assembly is an attractive and powerful strategy for fabricating supramolecular architectures.[1] Based on this concept, nanoscale structures can potentially be precisely manipulated by rational design and modification of the self-assembling building blocks at the molecular level. Nature has provided infinite examples which perfectly elucidate this concept. In the endoplastic reticulum, for example, the membrane structures can be elegantly regulated from tubes to vesicles by adjusting the concentration of curvature-shaping proteins in the multicomponent lipid bilayer.[2] To elucidate this unique feature of the natural self-assembly process, a variety of artificial building blocks have been designed. Among them, amphiphiles have proven to be an important type of building block, with the ability to bridge molecules and form nanostructures stabilized by different driving forces,[3] such as charge-transfer interactions, which have been extensively exploited to produce liquid crystal structures with high charge mobility.[4] Moreover, the shape and amphiphilicity of the building blocks can be readily tailored by forming supramolecular complexes, thus further manipulating the self-assembly architectures.[5] In this context, the structural regulation of tubes and vesicles by molecular coassembly, which is crucial to numerous cellular activities, has rarely been realized in artificial amphiphile systems.[6]

Herein, we report a successful manipulation of self-assembling nanostructures by noncovalent modification of amphiphiles, manipulated by charge-transfer interactions, which result in a transformation from fluorescent tubes to vesicles in aqueous media. For this purpose, 1-[11-oxo-11-(pyren-1-ylmethoxy)-undecyl]pyridinium bromide (PYR), containing an electron-rich pyrenyl group, and ethane-1,2-diyl bis(3,5-dinitrobenzoate) (DNB), with two electron-deficient dinitrobenzene units utilized as electron acceptors, were chosen as the two components (Figure 1). PYR and DNB can initially coassemble into a supramolecular complex driven by a charge-transfer interaction between the pyrenyl group of

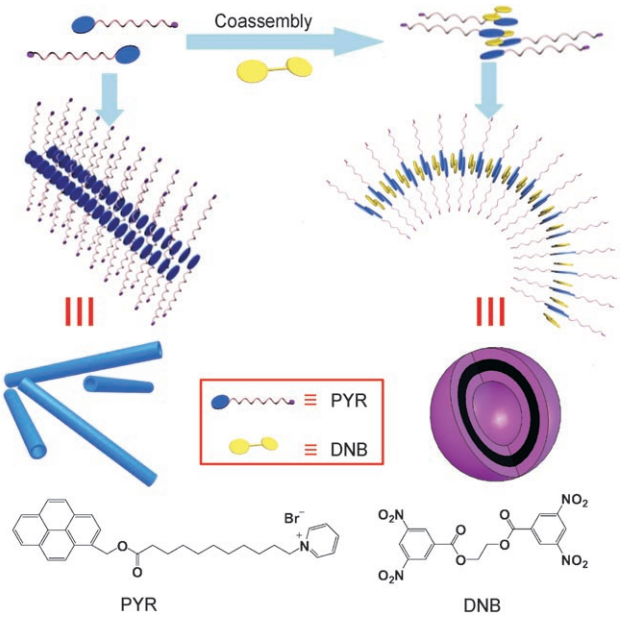

Figure 1. Schematic representation of the transformation from tubes to vesicles, and the molecular structures of PYR and DNB.

PYR and the dinitrobenzene groups of DNB.[7] In this way, the amphiphilicity and the shape of the building units can be altered, further influencing the self-assembly behavior in aqueous media.

Typically, the PYR–DNB complex was prepared by mixing PYR and DNB, in a molar ratio of 2:1, in THF, a good solvent for both PYR and DNB. The solvent was then removed under reduced pressure. The dissolution–evaporation procedure was repeated three times, to ensure complete complexation, and the resultant complex was dried at room temperature under reduced pressure. Interestingly, the pre-assembled complex was readily soluble in water, yielding a yellow transparent solution which was stable for several months. As uncomplexed DNB is insoluble in water, solubility can be attributed to its charge-transfer-driven complexation with PYR. Notably, PYR forms a colorless solution in water. The color change after addition of DNB is also a result of the complexation process. Further evidence for the formation of a stable charge-transfer complex was obtained from UV/Vis absorption and fluorescence emission spectroscopy. As is shown in Figure 2, the complex exhibits a broad absorption between 400 nm and 550 nm which corresponds to the characteristic absorption of the charge-transfer complex.[7] Concomitantly, drastic fluorescence quenching was also detected after complexation. A series of PYR–DNB complexes with different donor/acceptor ratios were also

[*] C. Wang, Dr. S. C. Yin, S. L. Chen, Dr. H. P. Xu, Prof. Z. Q. Wang, Prof. X. Zhang
Key Lab of Organic Optoelectronics & Molecular Engineering
Department of Chemistry, Tsinghua University
Beijing 100084 (P.R. China)
Fax: (+86) 10-62771149
E-mail: xi@mail.tsinghua.edu.cn

[**] This work was financially supported by the National Basic Research program (2007CP808000), the NSF (20574040, 50703022), and theNSFC-DFG joint grant (TRR61). We also acknowledge Prof. Changyou Gao at Zhejiang University for CLSM measurements.

Supporting information for this article is available on the WWW under http://dx.doi.org/10.1002/anie.200803361.

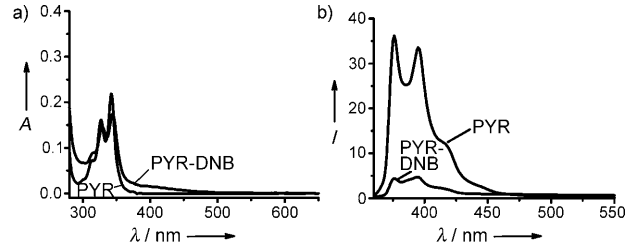

Figure 2. a) UV/Vis absorption spectrum and b) fluorescence emission spectrum of PYR and PYR–DNB complex. The solvent is water and the concentrations of PYR and DNB are 1.0×10^{-4} M and $5\times^{10-5}$ M, respectively.

prepared. As the DNB-content increased, the emission intensity decreased, without any change in the spectral pattern (see Supporting Information, Figure S4). No exciplex emission was detectable in the spectral region under these experimental conditions, indicating that the quenching process occurred by charge transfer from the pyrenyl units to the dinitrobenzoate units.

To investigate higher-order self-assembled aggregates in aqueous media, aqueous solutions of PYR and PYR–DNB complex (2:1 ratio) were prepared. The concentration of PYR in both of these solutions was 1×10^{-4} M, approximately two times higher than the critical aggregation concentration (CAC).

As indicated by the fluorescence microscopy images and confocal laser scanning microscopy (CLSM) images (Figure 3a–c), PYR self-assembled into rods of up to 20 micrometers in length (Figure 3b). At different concentrations above the CAC, the rods exhibited the same shape and similar size distribution. After complexation, no images for the PYR–DNB complex could be visualized due to the aforementioned fluorescence quenching effect. The rodlike structure of PYR was further confirmed by optical microscopy. As is shown in Figure 3d, the shape and size of the rods were consistent with those displayed by fluorescence microscopy and CLSM images. After complexation, however, spherelike aggregates were observed (Figure 3e), drastically different from the rodlike structures constructed by PYR alone.

A clearer indication of the self-assembly structures before and after complexation was provided by transmission electron microscopy (TEM). Analysis of PYR samples on carbon-coated grids revealed that the rodlike aggregates were tubular in structure, as evidenced by the clear contrast between the dark periphery and the lighter central part (Figure 4a). The

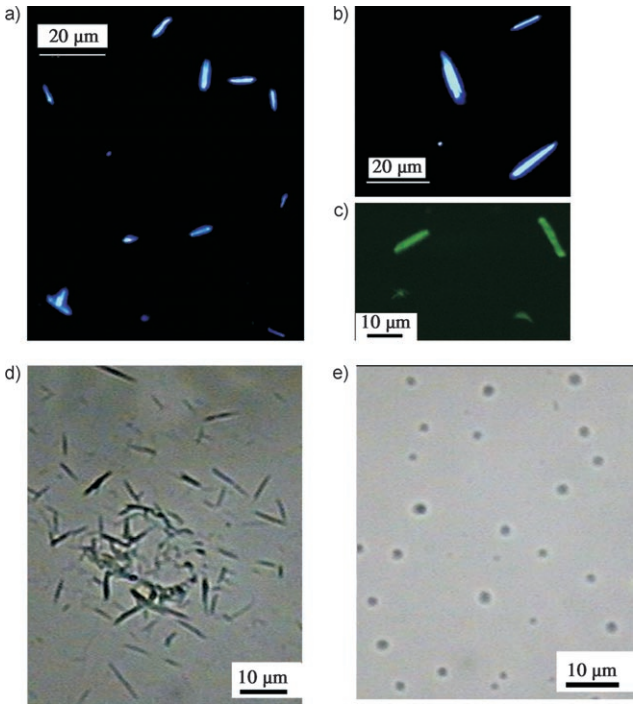

Figure 3. a, b) Fluorescence microscopy images of PYR aggregates; c) confocal laser scanning microscopy (CLSM) image of the PYR aggregates; optical microscopy images of d) PYR and e) PYR–DNB.

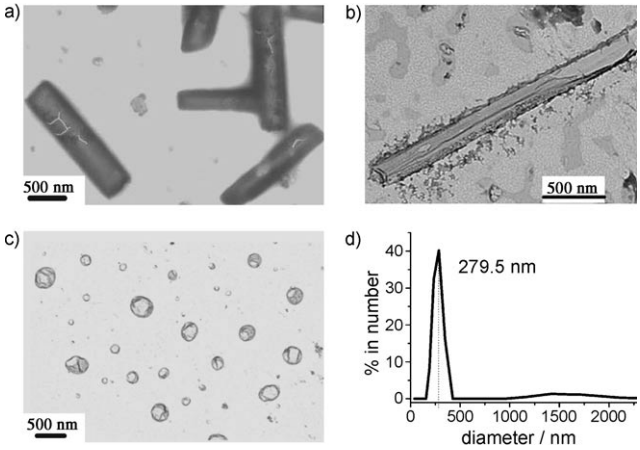

Figure 4. TEM images of a) PYR aggregates, b) one of the broken tubes and c) PYR–DNB aggregate; d) DLS data of PYR–DNB aggregate.

hollow nature of the assemblies could also be visualized for the broken aggregate shown in Figure 4b. Conversely, after complexation, the PYR–DNB complex displayed a typical vesicular structure. Optical microscopy revealed that the spheres were actually hollow (Figure 4c). The average size of the vesicles shown in the TEM images was about 300 nm, consistent with the dynamic laser scattering (DLS) results, which gave an average size of 279.5 nm.

A remarkable increase in stability is also apparent upon the formation of the charge-transfer interaction. Prior to complexation, the tubular structure was relatively unstable and gradually decomposed into amorphous aggregates over a period of two weeks. After complexation, however, the vesicular structure of PYR–DNB is maintained for several months.

UV/Vis spectroscopy and X-ray diffraction (XRD) were used to clarify the packing of PYR molecules in the tubular aggregates. Higher dilution leads to a blue shift (Figure 5a), indicating an *H*-aggregation form,[8] which suggests that adjacent pyrene aromatic rings undergo considerable overlap. The bilayer nature of the PYR membrane was revealed by XRD and small-angle X-ray scattering (SAXS) results, as

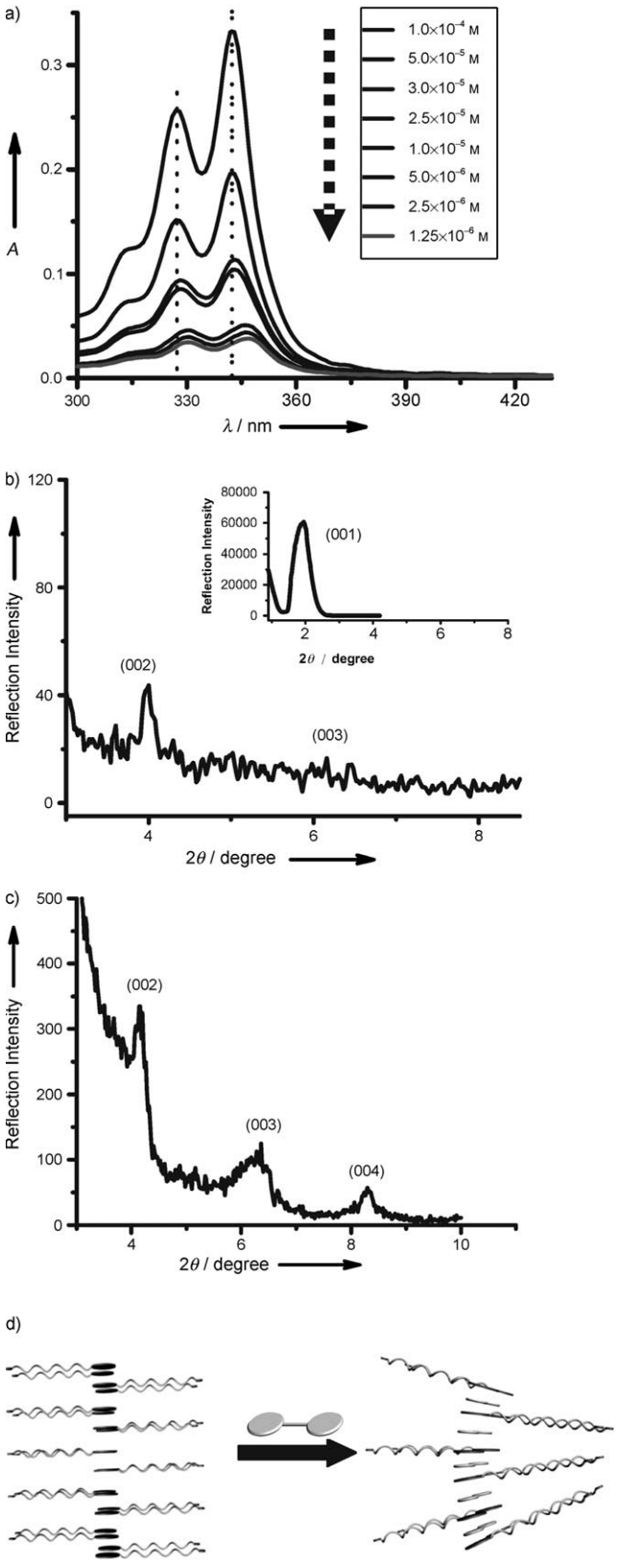

Figure 5. a) UV/Vis absorption spectra of aqueous solutions of PYR at different concentrations; b) XRD and (inset) SAXS scans of PYR; c) XRD scan of PYR–DNB; d) Schematic representation of the curvature-dependent mechanism.

shown in Figure 5b and c. The thickness of the bilayer was calculated to be 4.5 nm, in agreement with the length of two PYR molecules with antiparallel packing and overlapped pyrene rings. We then investigated whether the bilayer framework was maintained after complexation. According to the classical packing form,[4,9] the dinitrobenzyl group is inserted between adjacent pyrene groups to form an intercalated donor–acceptor structure, without changing the thickness of the bilayer. This structure was further confirmed by XRD results, with a bilayer thickness of approximately 4.5 nm retained.

A mechanism is proposed to explain why the shape of PYR aggregates transforms from tubes to vesicles after complexation with DNB. The shapes of the aggregates, formed by the two distinct lipid bilayers, are determined by the spontaneous curvature of the membrane.[10] Typically, the formation of tubular structures is dependent on high membrane curvature while a low-curvature membrane favors the formation of a vesicular structure.[11] Prior to complexation with DNB, PYR self-assembles in aqueous solution to form a highly ordered bilayer of packed pyrenyl groups with a strong tendency to stack together through π-electronic interactions, generating a high curvature and forming a tubular structure (Figure 5d). After complexation, the dinitrobenzyl groups are inserted into the PYR arrays. As a result of the polar nature of the dinitrobenzyl groups and the steric repulsion generated upon insertion, the straight PYR arrays along the axis become curved.[12] As a result, the high curvature for shaping the tubular structure is destroyed, topologically facilitating the formation of vesicles. Moreover, the DNB molecule serves as a "cross-linker" between the stacking arrays to enhance the stability of the vesicular aggregates.

To test the proposed mechanism, we undertook several control experiments. Firstly, the self-assembled structures of charge-transfer complexes with different PYR/DNB molar ratios were studied by TEM and DLS. TEM results revealed that the complexes with PYR/DNB ratios of 10:1 and 4:1 both exhibit vesicle structures but with differing size distributions (see Supporting Information, Figure S7a, b). DLS tests gave the average sizes of these vesicles as 519 nm and 374 nm, respectively, in contrast to the average size of 279.5 nm with a ratio of 2:1. These results indicated that the size of the vesicles decreased as the proportion of DNB in the mixture was increased. This trend can be attributed to the increase of intercalation, which leads to a more curved bilayer, and thus producing vesicles with smaller size.

Secondly, the electron-acceptor molecule was replaced by $C_6H_3(NO_2)_2CH_2OCOCH_3$ (SDNB), in which dinitrobenzoate groups were not covalently bonded to each other. A complex of PYR and SDNB in a 1:1 ratio (PYR–SDNB) was prepared. Formation of the complex was confirmed by the UV/Vis and the fluorescence emission spectra (see Supporting Information, Figure S6). The PYR–SDNB complex, with curvature induced by the intercalation of dinitrobenzene groups, was assumed to form vesicular aggregates, and this was revealed by TEM results (see Supporting Information, Figure S7c). According to TEM data, the vesicles have an average size of 250 nm, similar to that of PYR–DNB. However, the vesicles of PYR–SDNB are less stable than those of PYR–DNB.

Separate solutions of the two complexes were kept at room temperature for two weeks, after which time the remaining aggregates were inspected by TEM. The majority of the vesicles fabricated by PYR–SDNB collapsed into spherical micelles and branched tubes with many three-way junctions (see the Supporting Information, Figure S7d). In contrast, the vesicular structures of PYR–DNB were maintained even after one month (see Supporting Information, Figure S7e), thereby confirming the contribution of the linker moieties to vesicle stability. The above results support the proposed curvature-dependent mechanism.

The complex with a PYR/DNB ratio of 4:1 was also kept at room temperature for two weeks. Interestingly, TEM results show the remaining aggregates have budding vesicle morphologies (see Supporting Information, Figure S7f), as occur in intercellular traffic organelles in natural cells. The budding vesicle structure indicates a redistribution of the DNB component in the multicomponent membrane, generating different degrees of curvature in different domains.

In conclusion, we have demonstrated a novel example of self-assembly manipulated by charge-transfer interactions. In contrast to the tubular aggregates of PYR, the supramolecular charge-transfer complex PYR–DNB self-assembles into vesicles, induced by a curvature-dependent mechanism. The results exemplify the enormous potential of self-assembly for the construction of well-defined nanostructures by controlling the molecular building blocks. In addition, the manipulated morphogenesis presented here accords well with that which occurs in natural cellular membranes, which can also form vesicles, vesicle buds, branched tubules, and long, unbranched tubes, simply by varying the proportions of lipid and protein in the complex.[10] These findings provide a simple model that affords further understanding of the membrane deformation and micropatterning details in various cellular events. The possibility for continuous tube–vesicle transformations can potentially be used to fabricate artificial membranes with defined shape and controllable intervesicular transportation behaviors.

Experimental Section

XRD and SAXS analysis: One drop of sample solution (1×10–4 M) was placed onto a silicon surface and the solvent was evaporated at room temperature. This sample was used for XRD and SAXS measurements. The Bragg peak θ is extracted from the XRD data and the bilayer thickness d can then be obtained, according to the Braggequation $d = \lambda/(2 \sin\theta)$, $\lambda = 0.15405$ nm.

NMR spectra were recorded on a JEOL JNM-ECA300 spectrometer; ESI–MS was carried out on a PE Sciex API 3000 spectrometer. UV/Vis spectra were obtained using a Hitachi U-3010 spectrophotometer. TEM was performed on a JEMO 2010 electron microscope, operating at an acceleration voltage of 110 kV. The samples were prepared by drop-coating the aqueous solution on the carbon-coated copper grid. The fluorescent images were captured using a Bio-Rad Radiance 2100 CLSM.

Received: September 8, 2008
Published online: October 20, 2008

Keywords: aggregation · amphiphiles · charge transfer · self-assembly · vesicles

[1] a) J.-M. Lehn, *Supramolecular Chemistry*, VCH, Weinheim **1995**; b) G. M. Whitesides, M. Boncheva, *Proc. Natl. Acad. Sci. USA* **2002**, *99*, 4769 – 4774; c) D. Y. Chen, M. Jiang, *Acc. Chem. Res.* **2005**, *38*, 494 – 502; d) D. Y. Yan, Y. F. Zhou, *Science* **2004**, *303*, 65 – 67; e) P. Jonkheijm, E. W. Meijer, *Science* **2006**, *313*, 80 – 83.

[2] a) G. K. Voeltz, T. A. Rapoport, *Cell* **2006**, *124*, 573 – 586; b) G. K. Voeltz, M. M. Rolls, T. A. Rapoport, *EMBO Rep.* **2002**, *3*, 944 – 950.

[3] a) B. Song, Z. Q. Wang, S. L. Chen, X. Zhang, Y. Fu, M. Smet, W. Dehaen, *Angew. Chem.* **2005**, *117*, 4809 – 4813; *Angew. Chem. Int. Ed.* **2005**, *44*, 4731 – 4735; b) B. Song, S. L. Chen, Z. Q. Wang, X. Zhang, *Adv. Mater.* **2007**, *19*, 416 – 420; c) T. Kunitake, *Angew. Chem.* **1992**, *104*, 692 – 710; *Angew. Chem. Int. Ed. Engl.* **1992**, *31*, 709 – 726; d) J. H. Fuhrhop, T. Y. Wang, *Chem. Rev.* **2004**, *104*, 2901 – 2938.

[4] a) R. Keller-Griffith, H. Ringsdorf, *Colloid Polym. Sci.* **1986**, *264*, 924 – 935; b) H. Ringsdorf, J. Venzmer, *Angew. Chem.* **1988**, *100*, 117 – 162; *Angew. Chem. Int. Ed. Engl.* **1988**, *27*, 113 – 158; c) V. Percec, M. Glodde, T. K. Berra, Y. Miura, I Shiyanovskaya, K. D. Singer, V. S. K. Balagurusamy, P. A. Heiney, I. Schnell, A. Rapp, H.-W. Spiess, S. D. Hudson, H. Duan, *Nature* **2002**, *419*, 384 – 387; d) J. H. Wendorff, D. Janietz, *J. Mater. Chem.* **1998**, *8*, 265 – 274; e) M. Manickam, M. Belloni, *J. Mater. Chem.* **2001**, *11*, 2790 – 2800; f) N. Tchebotareva, K. Müllen, *J. Am. Chem. Soc.* **2003**, *125*, 9734 – 9739; g) E. Peeters, E. W. Meijer, *Chem. Eur. J.* **2002**, *8*, 4470 – 4474.

[5] a) Y. P. Wang, N. Ma, Z. Q. Wang, X. Zhang, *Angew. Chem.* **2007**, *119*, 2881 – 2884; *Angew. Chem. Int. Ed.* **2007**, *46*, 2823 – 2826; b) T. Kato, N. Mizoshita, *Angew. Chem.* **2006**, *118*, 44 – 74; *Angew. Chem. Int. Ed.* **2006**, *45*, 38 – 68; c) A. P. H. J. Schenning, E. W. Meijer, *J. Am. Chem. Soc.* **2001**, *123*, 409 – 416; d) N. Kunitake, T. Kunitake, *J. Am. Chem. Soc.* **1995**, *117*, 6360 – 6361; e) T. Kawasaki, N. Kimizuka, *J. Am. Chem. Soc.* **2001**, *123*, 6792 – 6800; f) Y. J. Jeon, K. Kim, *Angew. Chem.* **2002**, *114*, 4654 – 4656; *Angew. Chem. Int. Ed.* **2002**, *41*, 4474 – 4476.

[6] a) T. Furuya, S. Lee, T. Inoue, *Biophys. J.* **2003**, *84*, 1950 – 1959; b) S. Lee, H. M. Ellerby, *J. Biol. Chem.* **2001**, *276*, 41224 – 41228.

[7] a) D. Markovitsi, H. Ringsdorf, *J. Chem. Soc. Faraday Trans.* **1992**, *5*, 1741 – 1748; b) K. Naka, Y. Chujo, *Langmuir* **2003**, *19*, 5496 – 5501; c) Y. Shimazaki, M. Yamamoto, *Langmuir* **1997**, *13*, 1385 – 1387.

[8] M. Kasha, H. R. Rawls, *Pure. Appl. Chem.* **1965**, *11*, 371 – 392.

[9] a) O. Okabe, T. Aida, *Angew. Chem.* **2002**, *114*, 3564 – 3567; *Angew. Chem. Int. Ed.* **2002**, *41*, 3414 – 3417; b) D. Goldmann, D. Janietz, *Angew. Chem.* **2000**, *112*, 1922 – 1925; *Angew. Chem. Int. Ed.* **2000**, *39*, 1851 – 1854.

[10] a) H. T. McMahon, J. L. Gallop, *Nature* **2005**, *438*, 590 – 596; b) K. Farsad, P. De Camilli, *Curr. Opin. Cell Biol.* **2003**, *15*, 372 – 381.

[11] a) J. M. Schnur, *Science* **1993**, *262*, 1669 – 1675; b) T. Shimizu, M. Masuda, H. Minamikawa, *Chem. Rev.* **2005**, *105*, 1401 – 1443; c) J. B. Lee, H. G. Döbereiner, *Langmuir* **1999**, *15*, 8543 – 8545; d) V. H. S. Tellini, J. V. Tato, *Adv. Mater.* **2007**, *19*, 1752 – 1756; e) G. Boettcher, J. H. Fuhrhop, *Langmuir* **2001**, *17*, 873 – 877; f) K. Yu, A. Eisenberg, *Macromolecules* **1998**, *31*, 3509 – 3518; g) S. Vauthey, H. Y. Gong, *Proc. Natl. Acad. Sci. USA* **2002**, *99*, 5355 – 5360.

[12] N. J. Heaton, B. Herradón, *J. Am. Chem. Soc.* **1998**, *120*, 12371 – 12384.

